# DUAL-WAVELENGTH Q-SWITCHED FIBER LASER USING MECHANICALLY EXFOLIATED BLACK PHOSPHORUS AS A SATURABLE ABSORBER

M. B. HISYAM[a], A. A. LATIFF[b], M. F. M. RUSDI[a], Z. JUSOH[c], M. YASIN[d], S. W. HARUN[a,b*]

[a]*Department of Electrical Engineering, University of Malaya, 50603 Kuala Lumpur, Malaysia*

[b]*Photonics Research Centre, University of Malaya, 50603 Kuala Lumpur, Malaysia*

[c]*Faculty of Electrical Engineering, Universiti Teknologi Mara (Terengganu), 23000 Dungun, Terengganu, Malaysia*

[d]*Department of Physics, Faculty of Science and Technology, Airlangga University, Surabaya (60115) Indonesia*

We demonstrate a dual-wavelength Q-switched Ytterbium doped fiber laser (YDFL) using a newly developed multi-layer black phosphorous (BP) saturable absorber (SA). The BP SA is prepared by mechanically exfoliating BP crystal and fixing the acquired BP flakes onto the scotch tape. A small piece of the tape is then sandwiched between two ferrules and incorporated in cladding pumped YDFL cavity to achieve stable Q-switched operation at 1.0 μm region. The laser has a pump threshold of 816 mW, a pulse repetition rate tunable from 10.9 to 23.87 kHz, and a narrow pulsewidth of 9.3 μs. Our results show that multi-layer BP is a promising SA for Q-switching laser operation.

(Received April 16, 2016; Accepted July 4, 2016)

*Keywords:* Multi-layer black phosphorus, mechanical exfoliation, Q-switched laser, double-clad Ytterbium-doped fiber

## 1. Introduction

Passively Q-switched fiber lasers have attracted much attention in recent years due to their potential applications in many areas such as micromachining, metrology, medicine, telecommunications and fiber optical sensing [1-2]. Compared with the active technique, the passive Q-switching technique based on saturable absorber (SA) has significant advantages in terms of compactness, simplicity, and flexibility of implementation [3].Up to date, various SAs have been implemented, such as nonlinear polarization rotation (NPR) [4-5] semiconductor saturable absorber mirrors (SESAMs) [6], carbon nanotubes (CNTs) [7-8] and graphene [9] for Q-switching generation in various fiber lasers and cavities. However, due to certain intrinsic drawbacks of these SAs, such as environmental sensitivity, complex optical alignments, complicated fabrication and expensive packaging, or limited operating bandwidth, their applications are restricted. Therefore, there is constantly a strong motivation to seek new high-performance SAs for pulsed laser systems.

Most recently, black phosphorus (BP), a newly emerged 2D material, has also gained wide attention for potential application in developing the next-generation optoelectronics devices such as sensor, field-effect transistors and solar cells [10-12]. Stimulated by the similarity between graphene and BP in terms of single elemental component and direct band-gap, it is natural to find out whether BP could be used as a SA for the Q-switching and mode-locking applications. In this paper, we report what we believe to be the first demonstration of a passively Q-switched double-

*Corresponding author: swharun@um.edu.my

clad Ytterbium-doped fiber laser (YDFL) with multi-layer BP as a SA. Note that BP comprises only the elemental "phosphorus". Hence it could be easily peeled off by mechanical exfoliation. The proposed Q-switched YDFL also produces dual-wavelength output operating in the 1.09 μm wavelength region.

## 2. Preparation and characterization of Saturable Absorber

In this work, the BP based SA was prepared by mechanical exfoliation method, which has been widely used in graphene based ultra-fast fiber laser applications [13-14]. Mechanical exfoliation is advantageous mainly because of its simplicity and reliability, where the entire fabrication process is free from complicated chemical procedures and costly instruments. As shown in Fig. 1, relatively thin flakes were peeled off from a big block of commercially available BP crystal (purity of 99.995 %) using clear scotch tape. Then, we repeatedly pressed the flakes stuck on the scotch tape so that the BP flakes become thin enough to transmit light with high efficiency. Then we cut a small piece of the BP tape and attached it onto a standard FC/PC fiber ferrule end surface with index matching gel. After connecting it with another FC/PC fiber ferrule with a standard flange adapter, the all-fiber BP based SA was finally ready.

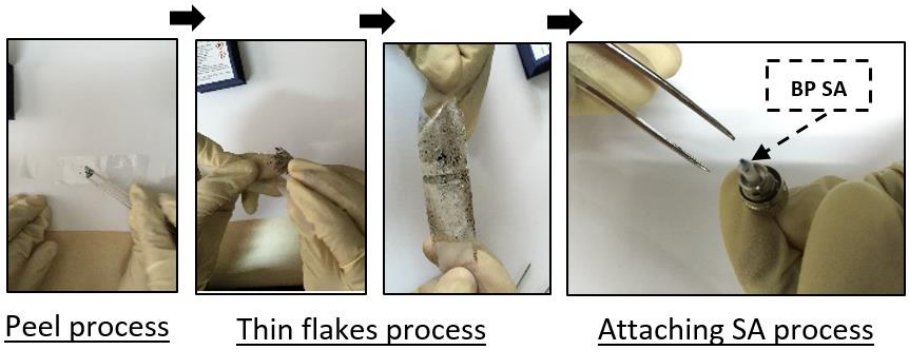


*Fig. 1 The preparation flow of BP-SA using mechanical exfoliation method.*

We verify the quality of the BP tape by using Field Emission Scanning Electron Microscopy **(**FESEM**)** as shown in Fig. 2(a). The FESEM image shows the existence of the uniform layers and confirms the absence of > 1μm aggregates or voids in the composite SA, which otherwise result in non-saturable scattering losses. The composition of the transferred layers is confirmed by the energy dispersive spectroscopy (EDS) on the FESEM image. The presence of BP material on the scotch tape adhesive surface was confirmed by presence of higher peak phosphorus in the spectroscopy data as shown in Fig. 2(b).We also performed Raman spectroscopy on the fabricated BP tape sample. Fig. 2(c) shows the Raman spectrum, which is recorded by a spectrometer when a 514 nm beam of a He-Ne laser is radiated on the tape for 10 ms with an exposure power of 10 mW. As shown in the figure, the sample exhibits three distinct Raman peaks at 360 $cm^{-1}$, 438 $cm^{-1}$ and 465 $cm^{-1}$ [15], corresponding to the$A_g^1$, $B_{2g}$ and $A_g^2$ vibration modes of layered BP. While the $B_{2g}$ and $A_g^2$ modes correspond to the in-plane oscillation of phosphorus atoms in BP layer, the $A_g^1$ mode corresponds to the out-of-plane vibration. The ratio between $A_g^1$ peak and silicon (Si) level at 520 $cm^{-1}$ estimates the thickness of BP flake as ~ 200 nm. The thickness for single-layer BP is about 0.8 nm [16], thus the prepared BP based SA is expected to consist of 250 layers.

The nonlinear optical response property for the multilayer BP on the scotch tape is then investigated to confirm its saturable absorption by applying an absorption technique. A self-constructed mode-locked fiber laser (1557 nm wavelength, 1.5 ps pulse width, 17.4 MHz repetition rate) is used as the input pulse source. The transmitted power and also a reference power for normalization are recorded as a function of incident intensity on the tape by varying the input

laser power. With increasing peak intensity, the material absorption decreases as shown in Fig. 2(d), confirming saturable absorption. The experimental data for absorption are fitted according to a simple two-level SA model [17];

$$\alpha(I) = \frac{\alpha_s}{1 + I/I_{sat}} + \alpha_{ns}$$

where $\alpha(I)$ is the absorption, $\alpha_s$ is the modulation depth, $I$ is the input intensity, $I_{sat}$ is the saturation intensity, and $\alpha_{ns}$ is the non-saturable absorption. As shown in Fig. 2(d), the modulation depth, non-saturable intensity, and saturation intensity are obtained to be 7 %, 58 % and 0.0025 MW/cm$^2$, respectively. Taking into account its nonlinear optical response leading to absorption saturation at relatively low fluence, the mechanically exfoliated BP meets basic criteria of a passive SA for fiber lasers.

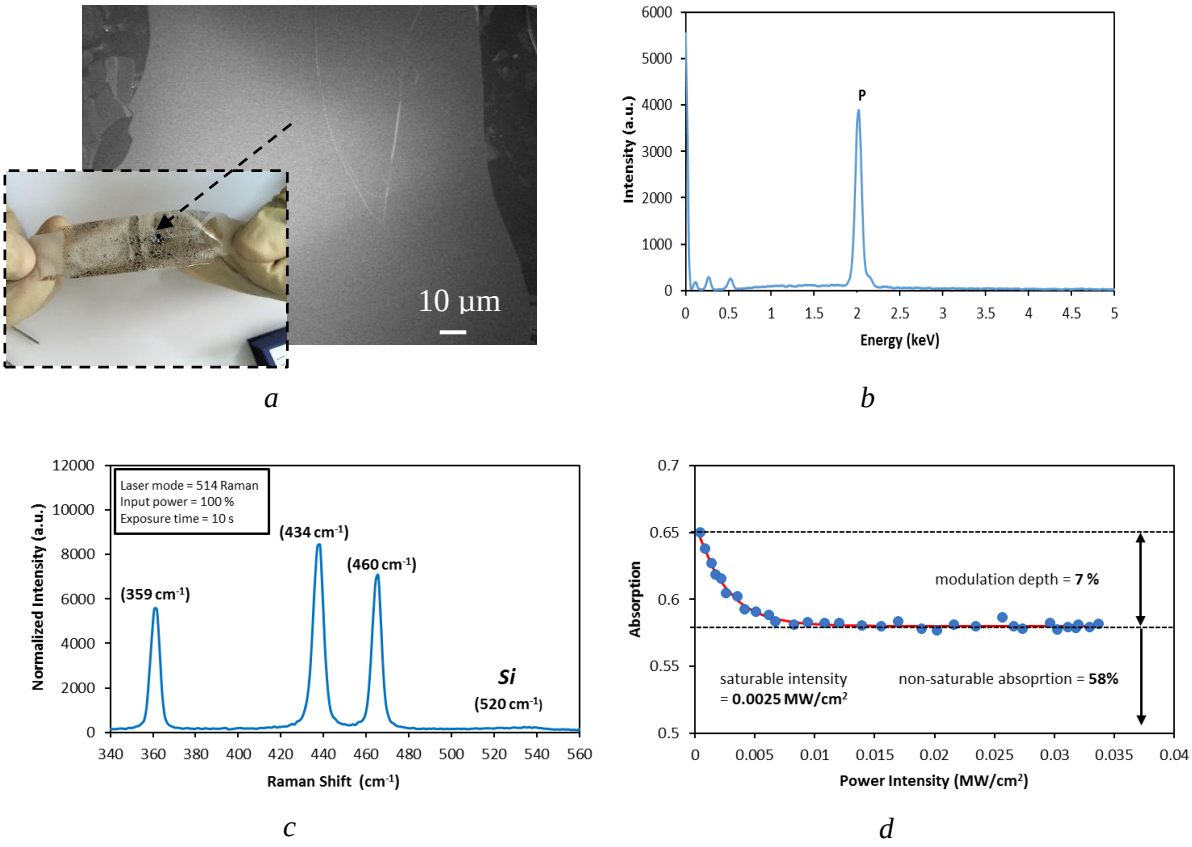


*Fig. 2 Material characteristics of the BP based SA (a) FESAM image of the BP tape. Inset shows the BP layer on a scotch tape. (b)EDS data for confirming the presence of phosphorus. (c) Raman spectrum of the multi-layered BP tape. (d) Nonlinear saturable absorption profile showing saturable absorption.*

## 3. Experimental setup

The fabricated SA is incorporated in the YDFL cavity for Q-switching generation as shown in Fig. 3. It uses a 10 m long double-clad Ytterbium-doped fiber (YDF) as a gain medium, which was pumped by a multimode 980 nm pump via a multimode combiner. The YDF has core diameter of 11 µm, cladding diameter of 130 µm, a numerical aperture of 0.46 and cladding absorption of 3.9 dB/m at 975 nm. The multilayer BP on the scotch tape acted as a passive Q-switcher. It was integrated into the fiber laser cavity by sandwiching a ~1 mm × 1 mm piece of the composite tape between two fiber connectors, adhered with index matching gel. It has to note that

the BP-SA is polarization-dependent due to anisotropic layered material characteristic [11]. So the polarization controller (PC) is employed to adjust the coupling of light from the fiber to the absorber. The signal was coupled out using 90:10 output coupler which keeps 90% of the light oscillating in the ring cavity for both spectral and temporal diagnostics. The laser output from the coupler was simultaneously monitored using a 500 MHz oscilloscope together with a 1.2 GHz photodetector, a 7.8 GHz radio-frequency (RF) spectrum analyzer and an optical spectrum analyzer (OSA) with a spectral resolution of 0.02 nm. The total length of the ring cavity is around 14.8 m.

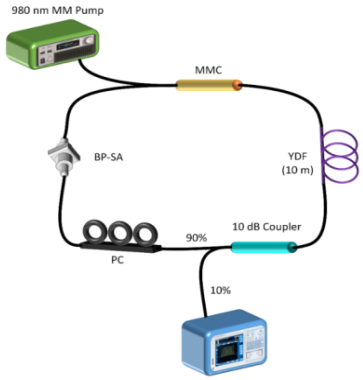


*Fig. 3 Configuration of the Q-switched YDFL setup employing a multi-layered BP on the scotch tape.*

## 4. Result and Discussion

The YDFL started to operate in the continuous-wave mode at the pump power of 750 mW, before transiting to the Q-switching operation at ~816 mW. As the pump power increased up to 1133 mW, a stable pulse train with an increasing repetition rate was observed. This is a typical feature of passive Q-switching whose characteristics at a multimode pump power of 1133 mW are presented in Fig. 4. The output optical spectrum in Fig. 4(a) displays two lasing wavelengths at 1088 nm and 1092 nm due to nonlinear polarization rotation (NPR) effect inside the cavity. When the double-clad YDF is pumped by a multimode 980 nm laser diode to generate population inversion of Ytterbium ions, an amplified spontaneous emission (ASE) is produced in 1 μm region via spontaneous and stimulated emission processes. The ASE oscillates in the ring cavity to generate laser when the gain overcomes the total cavity loss. With increasing power of the pump, dual-wavelength laser is generated due to the effect of the YDF birefringence, which induced phase variation in the ring laser cavity based on NPR effect. By adjusting the polarization state of the oscillating light, NPR can induce intensity-dependent loss (IDL) inside the ring cavity to alleviate mode competition caused by homogeneous broadening in the gain medium. Since, the YDF used in the cavity has a reasonably high nonlinearity, it produces sufficient NPR- and four-wave mixing (FWM)-induced IDL effect in the laser cavity. In this case, the transmission term varies too fast with the power and thus allows at least two wavelengths to oscillate in the ring cavity.

Fig. 4(b) shows the typical oscilloscope trace of the Q-switched pulse train which indicates the period of 42 μs without noticeable timing jitter. This corresponds to a repetition rate of 23.87 kHz. The pulse width is approximately 9.3 μs, which is comparable to the values obtained by other SAs. To verify that the passive Q-switching was attributed to the BP SA, the FC fiber ferrule filled with BP tape was replaced with a common clean ferrule. In this case, no Q-switched pulses were observed on the oscilloscope even when the pump power was adjusted over a wide range. This finding has confirmed that the BP-based SA was responsible for the passively Q-switched operation of the laser. Fig. 4(c) shows the corresponding RF spectrum at multimode pump power of 1133 mW. As seen in the figure, the fundamental repetition rate of the Q-switched pulses is 23.87 kHz which agrees with the pulse period of 42 μs measured in Fig. 4(b).The RF signal-to-noise ratio is observed at 57 dB, indicating that the passively Q-switching operation was

very stable. The dual-wavelength operation with 4 nm wavelength separation might interfere with one another, then inducing 250 MHz mode-beating frequency. Throughout the experiment, we can confirm that no mode-beating frequency presence.

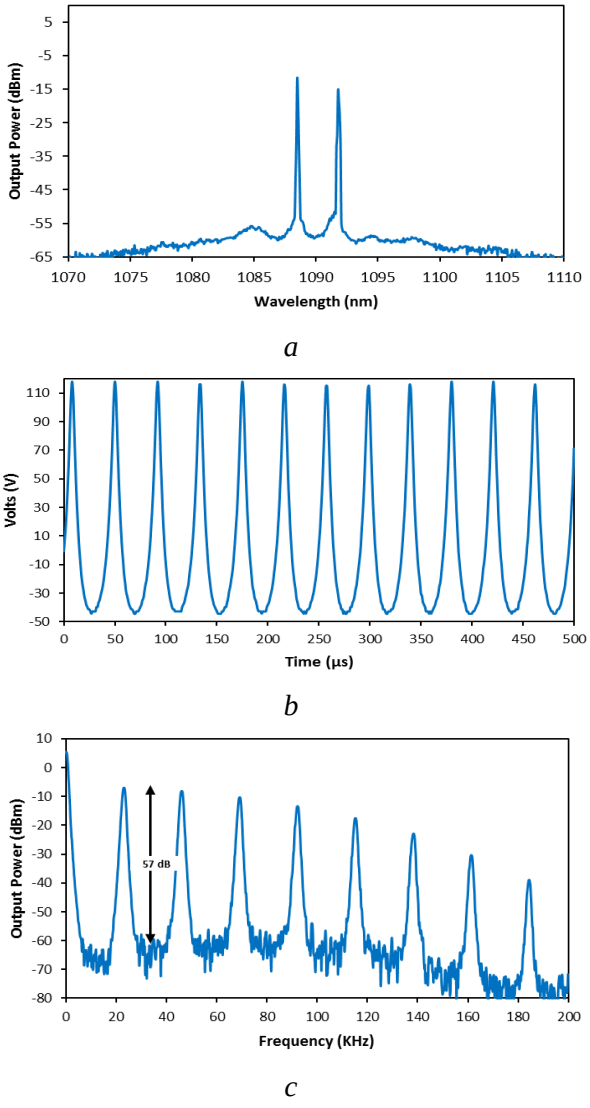


*Fig. 4 Output pulse characteristics of the Q-switched fiber laser at a multimode pump power of 1133 mW (a) output spectrum (b) typical pulse train (c) RF spectrum.*

Unlike the fixed repetition rate of a mode-locked fiber laser the pulse repetition rate in our laser increased with the pump power, which is a typical feature of passive Q-switching operation. Fig. 5 shows the pulse repetition rate and pulse width of the Q-switched fiber laser as functions of the incident pump power. By varying the multimode pump power from 816 to 1133 mW, the repetition rate of the Q-switching pulses can be increased from 10.9 to 23.87 kHz. Concurrently, the pulse width decreased from 13.56 to 9.3 µs. The pulse width could be decreased further by either shortening the cavity length or improving the modulation depth of the BP Q-switcher [18-19]. In addition, the average output power and the corresponding single-pulse energy are plotted against the pump power as shown in Fig.6.

It is observed that the average output power almost linearly increased with the input pump power up to the pump power of 1133 mW where the maximum average output power is 50 mW. The slope efficiency of the Q-switched laser is calculated to be around 9.66 %.One can see from the figure that the pulse energy linearly reduce in the initial stage, but after the pump power over

1000 mW, the pulse energy became to increase. The maximum pulse energy is 1.05μJ. We believe that the performance of Q-switched pulses produced by the laser could be further improved by optimizing the SA parameters of BP tape and the cavity design

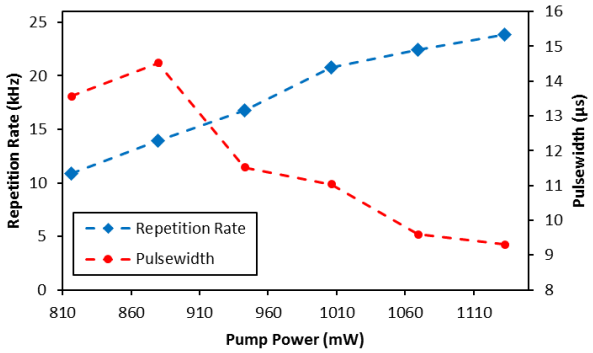


*Fig. 5 Pulse repetition rate and pulse width at different pump powers.*

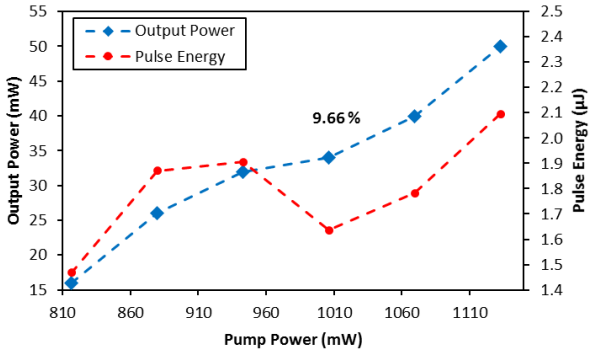


*Fig. 6 Average output power and pulse energy at different pump powers.*

## 5. Conclusion

We experimentally demonstrated a passively Q-switched ring YDFL using a multi-layer BP flakes onto a scotch tape as a SA. The tape with 250 layers of BP was prepared by the mechanical exfoliation method and sandwiched between two FCs with a fiber adapter to form a fiber-compatible BP-based SA. Stable Q-switched pulses at 1088 and 1092 nm were successfully obtained within the multimode pump power range from 816 mW to 1133 mW. At the maximum pump power, the laser showed the average output power, pulse energy, and pulse duration of 50 mW, 1.05 μJ, and 9.3 μs, respectively. The pulse repetition rate could be varied over a wide range of frequencies, from 10.9 to 23.87 kHz, by adjusting the pump power. Our experimental results suggest that multi-layer BP is a promising material for pulsed laser applications.

### Acknowledgement

This work is financially supported by Ministry of Higher Education Grant Scheme (FRGS/1/2015/SG02/UITM/03/3) and PPP University of Malaya Grant Scheme (PG098-2014B).

## References

[1] M. C. Pierce, S. D. Jackson, P. S. Golding, B. Dickinson, M. R. Dickinson, T. A. King, et al.,

"Development and application of fiber lasers for medical applications," in BiOS 2001 The International Symposium on Biomedical Optics, 2001, pp. 144-154.
[2] L. Shang, J. Ning and X. Yang, Optoelectron. Adv. Mater. - rapid commun., **4(**9), 1275 (2010).
[3] L. Pan, I. Utkin, and R. Fedosejevs, Photonics Technology Letters, IEEE, **19**, 1979 (2007).
[4] X. Yang, C. Yang, Laser physics, **19**, 2106 (2009).
[5] Z. C. Tiu, S. J. Tan, A. Zarei, H. Ahmad, S. W. Harun, Chinese Physics Letters, **31**,094206 (2014).
[6] H.-Y. Wang, W.-C. Xu, A.-P. Luo, J.-L. Dong, W.-J. Cao, L.-Y. Wang, Optics Communications, **285**, 1905 (2012).
[7] F. Ahmad, S. Harun, R. Nor, N. Zulkepely, F. Muhammad, H. Arof, et al., Journal of Modern Optics, **61**, 541 (2014).
[8] A. Tausenev, E. Obraztsova, A. Lobach, A. Chernov, V. Konov, P. Kryukov, et al., Applied Physics Letters, **92**, 171113 (2008).
[9] G. Sobon, J. Sotor, I. Pasternak, A. Krajewska, W. Strupinski, K. M. Abramski, Optics express, **21**, 12797 (2013).
[10] L. Li, Y. Yu, G. J. Ye, Q. Ge, X. Ou, H. Wu, et al., Nature nanotechnology, **9**, 372 (2014).
[11] F. Xia, H. Wang, and Y. Jia, Nature communications, vol. 5, 2014.
[12] M. Buscema, D. J. Groenendijk, G. A. Steele, H. S. van der Zant, A. Castellanos-Gomez, Nature communications, vol. 5, 2014.
[13] A. Martinez, K. Fuse, and S. Yamashita, Applied Physics Letters, **99**, 121107 (2011).
[14] K. S. Novoselov, V. Fal, L. Colombo, P. Gellert, M. Schwab, K. Kim, Nature, **490**, 192 (2012).
[15] S. Sugai, I. Shirotani, " Solid state communications, **53**, 753 (1985).
[16] A. Castellanos-Gomez, L. Vicarelli, E. Prada, J. O. Island, K. Narasimha-Acharya, S. I. Blanter, et al., 2D Materials, **1**, 025001 (2014).
[17] H. Mu, S. Lin, Z. Wang, S. Xiao, P. Li, Y. Chen, et al., Advanced Optical Materials, **3**, 1447 (2015).
[18] J. Zayhowski and P. Kelley, Quantum Electronics, IEEE Journal of, **27**, 2220 (1991).
[19] J. J. Degnan, Quantum Electronics, IEEE Journal of, **31**, 1890 (1995).